Oncolytic adenovirus H101 enhanced antitumor effects of PD-1 blockade by downregulating CD47 on tumor cells

Chenxiao Qiao
Institute of Immunology, Zhejiang University School of Medicine
Song Wang
Department of Urology, Zhejiang Cancer Hospital
Yipeng Xu
Department of Urology, Zhejiang Cancer Hospital
Yedie He
Department of Urology, Zhejiang Cancer Hospital
Zhijian Cai
Institute of Immunology, Zhejiang University School of Medicine
Hua Wang (wanghua@zjcc.org.cn)
Department of Urology, Zhejiang Cancer Hospital

Research Article

Keywords: Cancer, oncolytic adenovirus, macrophage, CD47, PD-1 blockade

Posted Date: April 19th, 2023

DOI: https://doi.org/10.21203/rs.3.rs-2823970/v1

Abstract

Programmed cell death protein 1/programmed cell death ligand 1 (PD-1/PD-L1) blockade are standard of care for many patients with advanced or metastatic cancer. However, a majority of patients remain resistant to these treatments. It has been reported that local oncolytic viral infection of tumors is capable of overcoming systemic resistance to PD-1 blockade, and strongly suggest the combination therapy of virotherapy with PD-1 blockade to improve therapeutic efficacy in tumors that are refractory to checkpoint blockade. We investigate the antitumor effects of an E1B55KD deleted oncolytic adenovirus H101, in combination with a humanized anti-PD-1 monoclonal antibody Camrelizumab on cancer. Combination of H101 with Camrelizumab demonstrated more potent antitumor effects than monotherapy in immune system humanized NSG mice subcutaneous (S.C.) tumor model. Increased tumor infiltrating T cells including the total and IFN-γ-expressing $CD8^+$ T cells in the combination treatment group were observed. H101 infection induced decreased expression of CD47 on cancer cells, thereby promoting macrophage to phagocytose cancer cells. With the activation of macrophage by H101, increased levels of cytokines including TNF, IL-12 and IFN-γ were observed when induced THP-1 cells were co-cultured with H101-treated cancer cells, which further induced increased expressions of IFN-γ in T cells. Eliminating the IL-12 by anti-IL-12 neutralizing antibodies abolished IFN-γ production from T cells, showing activation of macrophages by H101 induced oncolysis to promote IFN-γ secretion of T cells via IL-12. Meanwhile, infection with H101 induced upregulation of PD-L1 on YTS-1 cells. These results suggested that H101 works synergistically to enhance therapeutic efficacy of PD-1 blockade on cancer by suppressing CD47 signaling, which may promote phagocytose of macrophages to tumor cells and activate $CD8^+$ T cells. Combination of H101 with PD-1 blockade would be a novel strategy for treating cancer.

Introduction

Worldwide, an estimated 19.3 million new cancer cases and almost 10.0 million cancer deaths occurred in 2020 (1). Most patients with locally advanced or metastatic cancer are incurable with currently available treatments. Immune checkpoint inhibitors (ICIs) alone or in combination with conventional treatments, such as radiotherapy and chemotherapy have become an increasingly used therapeutic option for many patients with advanced or metastatic cancer (2). However, a majority of patients remain resistant to these treatments (3). Biomarkers to predict the response and development of combinatorial strategies to improve the efficacy of immunotherapy are needed to make therapy beneficial for a larger patient population. Several groups demonstrated that tumor response were correlated with expression of PD-L1 (4) and increase of tumour infiltrating $CD8^+$ T cells (5). Thus, to induce PD-L1 upregulation and/or attract $CD8^+$ T cells into tumors by altering the immune-suppressive tumor microenvironmen would be a strategy to enhance the efficacy of immune checkpoint blockade.

Oncolytic adenoviruses with deletion of E1B-55kD or mutated E1A are able to replicate selectively in, and kill cancer cells that have deficient p53 or disrupted Rb pathway while sparing normal cells, known as oncolytic virotherapy, are novel and promising potential treatments for cancer (6). However, a phase I/II

trial of ONYX-015 (an E1B55 KD-deleted adenovirus) delivered by injection into the primary tumor to treat pancreatic carcinomas showed modest antitumor activity especially used as a single agent although it is feasible and generally well tolerated either alone or in combination with gemcitabine (7). Meanwhile, an E1A mutated oncolytic adenovirus Delta-24-RGD has completed Phase I trials in patients with recurrent high-grade gliomas and showed the virus was well tolerated (8). In the past two decades, many preclinical studies demonstrated potent antitumor effects of oncolytic adenovirus on cancer, however, it has not fully translated into clinical applications in cancer due to limited therapeutic efficacy when applied as a monotherapy (9). Recently, it has been reported that oncolytic viruses induced lyse of infected cell can stimulate systemic antitumor immunity by release of danger associated molecular patterns (DAMPs), pathogen-associated molecular pattern molecules (PAMPs), and cytokines lead to maturation of antigen presenting cells (APCs), and then recruit $CD4^+$ and $CD8^+$ cells to destroy cells expressing viral antigens on tumors (10). Furthermore, Newcastle disease virus (NDV) induced PD-L1 upregulation in both infected tumors and in tumors not infected by virus, and intratumoral therapy with NDV sensitized the tumors to the efficacy of PD-1 and PD-L1 blockade in tumor models (11).

In the present study, we investigate the antitumor effects of H101, an E1B55KD and partial E3 deleted oncolytic adenovirus, which is the first and only adenovirus to be approved by the China State Food and Drug Administration in 2005 for treating head and neck cancer, in combination with a humanized anti-PD-1 monoclonal antibody Camrelizumab on cancer. Our study found that H101 infection induced downregulation of CD47 on infected cancer cells, which promote macrophage to phagocytose cancer cells. In vivo, combination therapy of H101 with Camrelizumab demonstrated potent antitumor effects than single agent alone in mice S.C. tumor model. By analyzing tumors treated, we found that increased tumor infiltrating T cells, especially, IFN-γ-expressing $CD8^+$ T cells in the combination treatment group. Furthermore, increased expressions of cytokines including TNF, IL-12 and IFN-γ were observed in H101 treated or combination treated tumor tissues. These results suggest that H101 indirectly activate macrophages and then induce the activation of T cells.

Materials And Methods

Cell lines

Human astrocytoma cell line U87-MG, human myeloid leukemia mononuclear cells THP-1, human bladder cancer cell line T24 were purchased from the American Type Culture Collection (Manassas, VA, USA). Human bladder cancer cell line YTS-1 (12, 13) was provided by the Department of Urology, Tohoku University School of Medicine (Sendai, Japan). T24 and YTS-1 cells were cultured in RPMI-1640 medium added with 10% fetal bovine serum (FBS) and 1% antibiotics (100 U/mL penicillin, 100 μg/mL streptomycin sulfates). U87-MG cells were cultured in Dulbecco's modified Eagle's medium (DMEM) supplemented with 10% FBS and 1% antibiotics. THP-1 cells were cultured in RPMI-1640 medium supplemented with 10% FBS, 1% antibiotics and β-mercaptoethanol (0.05mM). Induced THP-1 cells were stimulated with 50 ng ml^{-1} phorbol 12-myristate 13-acetate (Sigma-Aldrich, P8139) for 12 hours to

induce M0 macrophages. All cells were maintained in humidified incubator at 37℃ with 5% (vol/vol) CO_2.

Recombinant adenovirus

H101, a recombinant type 5 human adenovirus (also known as Oncorine) with a deletion of E1B55KD and partial E3 region (14) was provided from Shanghai Sunway Biotech Co., Ltd. Viruses were transfected into HEK293 cells to produce adenoviruses and the viral titer was determined by a standard plaque assay.

PD-1 inhibitor

Camrelizumab (SHR-1210) is a humanized IgG4 monoclonal anti-programmed cell death protein 1 (PD-1) antibody (15) that was provided by Jiangsu Hengrui Pharmaceutical Co., Ltd.

Western Blot Analysis

Cells were collected and washed with ice-cold PBS for 2 times. Then cells were lysed by RIPA lysis buffer (Beyotime, P0013B) added with 1mM PMSF on ice for 30 min.

The cell lysates were separated by sodium dodecyl sulfate-polyacrylamide gel electrophoresis (12%), transferred onto PVDF membranes (Millipore, ISEQ00010). The membranes were blocked with 5% BSA in PBST buffer and incubated with anti-CAR (Proteintech, 11777-1-AP) or anti-GAPDH (Abways Technology, AB0036) antibody at 4℃ overnight. The next day, the membranes were washed with PBST buffer for 3 times and incubated with Goat Anti-Rabbit IgG(H + L) HRP antibody (MultiSciences Biotech Co., Ltd, GAR007) for 1h at room temperature. The chemical signal was developed by UltraSignal ECL Western Blotting Detection Reagent (4A Biotech, 4AW011-1000). Then the membrane was scanned using Tanon 4500 Gel Imaging System.

Cell apoptosis assay

U87-MG, YTS-1 or T24 cells were collected and washed with PBS. Cell apoptosis were performed by Annexin V-APC/PI apoptosis kit (MultiSciences Biotech Co., Ltd, AP107) according to manufacturer's instructions.

Animal Studies

NSG mice (female, 6 weeks old) were purchased from GemPharmatech Co., Ltd (Jiangsu, China). Mice were housed under specific pathogen-free conditions, and the experimental protocols were approved by the Animal Care and Use Committee of the School of Medicine at Zhejiang University. In vivo treatments, mice were injected subcutaneously 3×10^6 U87-MG, 5×10^6 T24 or YTS-1 cells on day 0. Tumor-bearing mice received H101 treatments (2.5×10^7 pfu per tumor) via intratumoral injection every 2 days when tumor volume reached 100 mm^3. For the combination therapy, tumor-bearing mice received oncolytic virus treatment (2.5×10^7 pfu per tumor) via intratumoral injection every 2 days and/or received 50μg Camrelizumab treatment every 4 days when tumor volume reached 300 mm^3. In some experiments, NSG mice were intratumorally injected with 1×10^6 PBMCs isolated from peripheral blood of healthy donors.

PBMCs were isolated with Lymphocyte Separation Medium (TBDsciences, LTS1077) according to manufacturer's instruction. Tumor sizes were measured by Vernier calipers every 2 days and tumor volume was calculated by the following formula: volume = largest dimension × smallest dimension^2 × 0.5.

Immunofluorescence and confocal microscopy

Tumor tissues were isolated on day 14 after inoculating. The tissues were embedded in Tissue-Tek® O.C.T. Compound. Then, 10-μm-thick sequential frozen sections were cut using CryoStar NX50 (Thermo Fisher). Then the sections were fixed by -20°C prechilled methyl alcohol for 10 min and permeabilized by 0.1% Triton-X-100. After blocking with 5% BSA and 3% goat serum in PBS. Primary antibodies anti-CD8 (proteintech, 60181-1-Ig) and anti-IFN-γ (proteintech, 15365-1-AP) were incubated overnight at 4°C. The next day, cells were washed with PBS 3 times, and incubated with IFLUOR™ 488-(HUABIO, HA1211) and IFLUOR™ 549- (HUABIO, HA1126) labeled secondary antibodies for 30 min at room temperature. After washing 3 times with PBS, stained nuclei with DAPI (Invitrogen, D3571). The fluorescence signals were detected by Olympus IX83 FV3000 confocal microscope.

Quantitative real-time PCR

Total RNA was extracted from cells using RNAiso plus (TAKARA, 9109). 600ng RNA was reverse-transcribed into complementary DNA (cDNA) with the HiScript® II Q RT SuperMix (Vazyme Biotech co., ltd, R223-01) following the manufacturer's instructions. Real-time PCR was conducted using ChamQ Universal SYBR qPCR Master Mix (Vazyme Biotech co., ltd, Q711-02) and performed with CFX96 Touch Real-Time PCR Detection System (Bio-Rad). The following thermal cycling conditions were used for PCR: 1 cycle at 95°C for 30 s, followed by 40 cycles at 95°C for 5 s and 60°C for 34 s. The data were analyzed by the $2^{-\Delta\Delta Ct}$ method.

Phagocytosis assay

Tumor cells were stimulated with oncolytic viruses at MOI of 1 for 24 h before being collected. The cells were stained with CFSE (Invitrogen, C34570) according to manufacturer's instructions. CFSE-labeled cells were seeded into 6-well plates and co-cultured with induced THP-1 cells at 3:1 ratio. After 8 hours, all cells were collected and stained with anti-human CD45 (BioLegend, 982304) to distinguish induced THP-1 from tumor cells. Then CFSE-labeled CD45$^+$ induced THP-1 cells were detected by CytoFlex flow cytometer (Beckman Coulter, Brea, CA, USA). In some experiments, anti-CD47 (Bio X cell, BE0019-1) were added into the medium at a concentration of 10μg/ml.

Measurement of cytokine levels

The concentrations of cytokine levels of induced THP-1 and tumor tissue were analyzed by ELISA kits according to manufacturer's protocols. ELISA kits for human IFN-γ (430104), IL-12 (431704), TNF-α (430204), were purchased from BioLegend.

Flow cytometry

Cells were collected and washed 3 times with PBS. After stained by antibodies of surfaces markers, cells were permeabilized by IC Fixation Buffer (Thermo Fisher Scientific) and stained for the detection of intracellular cytokine. Flow cytometry was performed on CytoFlex flow cytometer (Beckman Coulter, Brea, CA, USA) and data were analyzed by FlowJo software (TreeStar Ashland, OR, USA). The following antibodies were used in staining cells: Fixable Viable Dye eFluorTM 520 (Invitrogen,65-0867-14), phycoerythrin-conjugated anti-human CD8a (BioLegend, 301007) and allophycocyanin-conjugated anti-human IFN-γ (BioLegend, 502511), allophycocyanin-conjugated anti-human CD45 (BioLegend, 982304).

Immunohistochemistry (IHC) analysis

Tumor tissues were isolated on day 7 after treatment. The Paraformaldehyde-fixed paraffin-embedded murine tumor tissue samples were sectioned (4 μm) and subjected to IHC staining with anti-IFN-γ (proteintech, 15365-1-AP) according to the manufacturer's instructions. Images of the sections were acquired with BX63 Olympus microscope.

Statistical analysis

All statistical analyses were performed using GraphPad Prism 8.0 software. All data are expressed as the mean ± s.d. values. Unpaired Student's t test was used to compare differences between the two groups. One-way ANOVA followed by the Newman–Keuls test was used to compare differences among multiple groups. The log-rank test was used for survival analysis, and the Spearman rank-order correlation test was used for Pearson correlation analysis. A difference was considered significant if the P-value was < 0.05.

Results

H101 inhibit tumor growth in a CAR-dependent manner

As CAR plays a key role in adenoviral infection and adenovirus induced oncolysis on target cells (16), we used CAR-positive and CAR-negative cancer cell lines in the study. As shown in Fig. 1a, U87-MG cells has a high expression of CAR, T24 cells has a moderate expression of CAR, while YTS-1 cells has little expression of CAR. As expected, H101 induced apoptosis of U87-MG and T24 cells in a dose-dependent manner and U87-MG showed higher apoptosis (Fig. 1b). However, H101 had no effect on the apoptosis of CAR-negative cell line YTS-1 (Fig. 1b). Consistent with these results, H101 significantly inhibited the growth of U87-MG and T24 tumors and prolonged the survival of the corresponding tumor-bearing mice (Fig. 1c, d). However, H101 did not give an antitumor effects on YTS-1 tumor-bearing mice (Fig. 1c, d). These results indicate that the H101 inhibit the tumor growth depending on their CAR expression.

H101 synergize with anti-PD1 to enhance the antitumor immunity

We next investigated whether H101 and anti-PD-1 have synergistic effects on tumor suppression. We established U87-MG, T24 and YTS-1 tumor model NSG mice and these mice were simultaneously

intratumorally injected with human peripheral blood mononuclear cells (PBMCs). H101 treatment significantly inhibited the CAR-positive cells U87-MG and T24 tumor growth, while anti-PD-1 treatment inhibited the growth of all tumor models (Fig. 2a). Importantly, combination therapy of H101 with anti-PD-1 produced more potent antitumor effects than single agent alone in all the tumor models tested (Fig. 2a). In addition, combination therapy prolonged the survival of all tumor-bearing mice (Fig. 2b). Immunofluorescence results revealed that combination therapy apparently enhanced the total and IFN-γ-expressing $CD8^+$ T cells in tumor tissues (Fig. 2c). These data suggest that H101 synergize with anti-PD1 to enhance the antitumor immunity.

H101 promote the macrophage phagocytosis by inhibiting CD47 expression

Then, we sought to explore how H101 improve the antitumor effects of anti-PD-1. We first detected the expression of some immune-related markers on U87-MG and YTS-1 cells after H101 treatment and found that the expression of FAS, HLA-A and ICAM1 did not altered (Fig. 3a). Subsequently, we detected the mRNA levels of PECAM and CD47 (responsible for “don’t eat me” signal of phagocytes) on H101 treated-U87-MG and YTS-1 and found CD47 rather than PECAM expression was significantly reduced (Fig. 3a). We further confirmed that CD47 protein level were decreased on both U87-MG and YTS-1 cells (Fig. 3b, 3c). CD47-mediated inhibition of macrophage phagocytosis leads to the loss of the first line of defense against cancer cells (17). Therefore, we supposed that H101 probably improve antitumor effects of anti-PD-1 by promoting macrophage phagocytosis of tumor cells. We induced THP-1 cells differentiated into M0 macrophages and found that H101 promoted induced THP-1 cells to phagocytize U87-MG and YTS-1 cells (Fig. 3d, 3e). Then we neutralized CD47 with anti-CD47 and found that oncolytic viruses could no longer increase the phagocytosis rate (Fig. 3f). These data suggest that H101 inhibited CD47 expression of tumor cells surface, thereby promoting macrophages to phagocytize more tumor cells.

T cells are activated by macrophages activated by H101-treated tumor cells

Subsequently, we examined whether increased phagocytosis of tumor cells can promote macrophage activation, thereby enhancing anti-PD-1 effects. We found that induced THP-1 cells, co-cultured with H101-treated U87-MG and YTS-1 cells secreted increased levels of cytokines including TNF, IL-12 and IFN-γ (Fig. 4a). After stimulated with supernatants from these cells, $CD8^+$ T cells released elevated IFN-γ (Fig. 4b). Then, we detected TNF, IL-12 and IFN-γ in tumor tissues and found that the levels of these cytokines also significantly increased in the lysates of tumor tissues from U87-MG and YTS-1 tumor-bearing mice with combination therapy (Fig. 4c). Moreover, the immunohistochemical results also detected the increased IFN-γ in the YTS-1 tumor tissues from mice with combination therapy (Fig. 4d). These results suggest that H101 indirectly activate macrophages and then induce the activation of T cells.

Macrophage-derived IL-12 is responsible for IFN-γ secretion from T cells

IL-12 plays an essential role in the induction of IFN-γ in T cells (18). So, we determined whether macrophages activated by H101-treated tumor cells can promote IFN-γ secretion from T cells via IL-12. Actually, we found that anti-IL-12 neutralizing antibodies (anti-IL-12) abolished IFN-γ production from T cells induced by macrophages phagocytizing H101-treated U87-MG and YTS-1 cells (Fig. 5a). Although IFN-γ is responsible for the upregulation of PD-L1 on tumor cells (19), we found that H101 could directly upregulate PD-L1 in infected YTS-1 cells (Fig. 5b). Therefore, H101 probably cause PD-1 signaling activation in T cells, which supports the necessity of the application of anti-PD-1 after H101 treatment.

Discussion

Oncolytic virus induced antitumor immune response make it an attractive immunotherapeutic agent for cancer therapy (20). Previous studies have shown that oncolytic virus has the potential to overcome resistance to immune checkpoint blockade (ICB) (21). Furthermore, combination of oncolytic virus with immune checkpoint blockade have shown great promise in the treatment of solid tumors although the mechanism by which oncolytic virus induces antitumor immunity is still being explored (22). In the present study, we investigated the antitumor effects of an oncolytic adenovirus H101 in combination with PD-1 inhibitor (Camrelizumab) on cancer in a humanized immune system mouse model. Our results demonstrated that combination therapy of H101 with Camrelizumab results in more significant tumor growth suppression than either agent alone. As virus induced antitumor immune arise from highly destructive nature of virus infection within the tumor by release of cellular danger signals and tumor antigens (23). We assessed virus-induced cytopathic effects of cancer cell lines by apoptosis analysis. Our results demonstrated that H101 induced apoptosis in CAR-positive cell lines U87-MG and T24, but not in CAR-negative cell line YTS-1. It is well known that CAR plays a key role in adenoviral infection, cancer cells with little expression of CAR would resistant to adenoviral infection and oncolysis (16). H101 inhibited tumor growth and prolonged survival in CAR-positive subcutaneous tumor model administrated intratumorally. However, CAR-negative tumor model were resistant to H101 treatment. Importantly, regardless of the CAR, combination of H101 with systemic PD-1 blockade resulted in synergistic tumor growth inhibition and prolonged the survival of tumor-bearing mice, when compared with each agent alone. Immunofluorescence analysis revealed more increased IFN-γ-expressing $CD8^+$ T cells in combination treatment group than H101 or PD-1 blockade treated tumor, confirming enhanced antitumor response exerted by IFN-γ-expressing $CD8^+$ T cells. These results suggest that H101 infection recruit $CD8^+$ T cells into tumor microenvironment (TME) and PD-1 blockade further activate $CD8^+$ T cells to attack tumor. It has been reported tumor infiltrating T cells are associated with response to anti-PD-1 treatment, patients without respond to PD-1 blockade therapy were more likely to lack CD8 + T cells inside the tumor lesions (24). The strategy to attract $CD8^+$ T cells into tumors by oncolytic virus may improve the antitumor activity of PD-1 blockade therapy. Thus, H101 in combination with PD-1 blockade are promising strategy for cancer immunotherapy. Previous studies reported that oncolytic virus induced upregulation of PD-L1 in TME, and thereby synergizes with anti-PD-L1 treatment leading to better therapeutic efficacy (25, 26). Another study demonstrated that localized oncolytic infection abrogated

resistance to systemic anti-PD-1 immunotherapy by upregulating PD-L1 on tumor cells and by eliciting a broad-range T-cell attack against the neoantigen (27).

The mechanism of virus-triggered antitumor immune response needs to be further elucidated. We detected immune-related markers in H101 treated cells and found viral infection resulted in downregulation of CD47 in infected cancer cells, which promoted THP-1 cells induced phagocytosis of cancer cells. Our results suggest, for the first time to our knowledge, that H101 may promote phagocytosis of macrophages to viral infected tumor cells by inhibit CD47 on tumor cells surface. It is well known CD47 plays an important role in tumor escape from macrophage-mediated phagocytosis (28). Thus, to block CD47 expressions on cancer cells would enhance the antitumor immune response. The strategies targeting CD47 including anti-CD47 antibody (29) and knockdown of CD47 (30) for cancer therapy have shown that CD47 blockade significantly increased macrophage infiltration and phagocytosis, thereby enhancing the antitumor response. As CD47 is also presence on normal cells, anti-CD47 antibodies could kill normal cells and cause possible off-target effects, such as anemia, thrombocytopenia, and leukopenia, limiting its clinical use (31, 32). Whereas H101 induced inhibition of CD47 occurs only in tumors due to selective replication of H101 in tumor cells. It has been reported that macrophages can prime $CD8^+$ T cell responses in mice upon CD47 blockade (33). We presumed that downregulation of CD47 by H101 would activate the T cell immunity by macrophages. We evaluated the effect of macrophage-mediated T cell responses on H101 treated cells, and found that co-culture of induced THP-1 cells with H101-treated cancer cells produced an increased expression of cytokines including TNF, IL-12 and IFN-γ. Furthermore, addition of supernatant from the macrophages to $CD8^+$ T cells, we observed the elevated expression of IFN-γ. Likewise, the increased levels of TNF, IL-12 and IFN-γ were observed in tumor tissues treated with H101 or PD-1 blockade, and combination of H101 with PD-1 blockade resulted in more further increase of those cytokines than that in single agents treated tumors. These results confirm the macrophage-mediated activation of $CD8^+$ T cells by both H101 or PD-1 blockade. As macrophages express PD-1, activation of PD-1 signaling on tumor associated macrophages by PD-L1 may suppress the ability of PD-1 + macrophages to phagocytose tumor cells (34). PD-1 blockade would promote phagocytose of macrophages to tumor cells and activate $CD8^+$ T cells. The strategies to combine immune checkpoint PD-1/PD-L1 blockade with innate immune checkpoint CD47/SIRPα blockade are promising for cancer immunotherapy (35–37). Our study demonstrated that combination therapy of H101 with PD-1 blockade significantly inhibited tumor growth and prolonged survival in a humanized immune system mouse tumor model. As IL-12 plays an essential role in the induction of IFN-γ in T cells (18). We determined whether macrophage-derived IL-12 is responsible for IFN-γ secretion in T cells, we found that remove of macrophage derived IL12 by anti-IL-12 neutralizing antibodies abolished IFN-γ from T cells. These results showed that macrophages derived IL12 induced IFN-γ secretion in T cells. It has been reported that IFN-γ may induce the upregulation of PD-L1 on tumors (19). Interestingly, we found that H101 infection induced upregulation of PD-L1 on YTS-1 cells with mechanism of uncertainty, which caused PD-1 signaling activation in T cells, supporting the combined therapy with PD-1 blockade. Several reports also demonstrated that infection with oncolytic viruses led to the upregulation of PD-1 in tumor cells and tumor-infiltrating immune cells, and combination therapy of

intratumorally administered oncolytic viruses and systemic PD-1 or PD-L1 blockade resulted in a marked enhancement of the antitumor immune effect, leading to rejection of the oncolytic virus-treated and distant, noninfected tumors (25, 38).

In conclusion, our study demonstrated that H101 works synergistically to enhance therapeutic efficacy of PD-1 blockade on cancer by suppressing CD47 signaling, which may promote phagocytose of macrophages to tumor cells and activate $CD8^+$ T cells. These findings support the important clinical implications of combination therapy with H101 and PD-1 blockade in cancer immunotherapy.

Declarations

DATA AVAILABILITY STATEMENT

The data that support the findings of this study are available on request from the corresponding author.

FUNDING

This work was supported by Techpool Bio-Pharma Co., Ltd (AKR-S005).

AUTHOR CONTRIBUTIONS

C.Q., S.W. conducted experiments.Y. X., Y.H. provided data analysis. Z.C.. provided academic advice and proofread the manuscript. H.W. wrote and edited the manuscript.

DECLARATION OF INTERESTS

All authors declare no competing interests.

References

1. Sung, H., Ferlay, J., Siegel, R.L., Laversanne, M., Soerjomataram, I., Jemal, A., Bray, F. (2021). Global cancer statistics 2020: GLOBOCAN estimates of incidence and mortality worldwide for 36 cancers in 185 countries. CA. Cancer. J. Clinic. 71, 209–249.
2. Barbari, C., Fontaine, T., Parajuli, P., Lamichhane, N., Jakubski, S., Lamichhane, P., Deshmukh, R.R. (2020). Immunotherapies and Combination Strategies for Immuno-Oncology. Int. J. Mol. Sci. 21, 5009.
3. Paucek, R.D., Baltimore, D., Li, G. (2019). The Cellular Immunotherapy Revolution: Arming the Immune System for Precision Therapy. Trends. Immunol. 40, 292-309.
4. Sadeghi Rad, H., Monkman, J., Warkiani, M.E., Ladwa, R., O'Byrne, K., Rezaei, N., Kulasinghe, A. (2021). Understanding the tumor microenvironment for effective immunotherapy. Med. Res. Rev. 41, 1474-1498.

5. Li, A., Chang. Y., Song. N.J., Wu. X., Chung. D., Riesenberg, B.P., Velegraki, M., Giuliani, G.D., Das, K., Okimoto, T., et al. (2022). Selective targeting of GARP-LTGFβ axis in the tumor microenvironment augments PD-1 blockade via enhancing CD8+ T cell antitumor immunity. J. Immunother. Cancer. 10, e005433.
6. Watanabe, M., Nishikawaji, Y., Kawakami, H., Kosai, K.I. (2021). Adenovirus Biology, Recombinant Adenovirus, and Adenovirus Usage in Gene Therapy. Viruses. 13, 2502.
7. Hecht, J.R., Bedford, R., Abbruzzese, J.L., Lahoti, S., Reid, T.R., Soetikno, R.M., Kirn, D.H., Freeman, S.M. (2003). A phase I/II trial of intratumoral endoscopic ultrasound injection of ONYX-015 with intravenous gemcitabine in unresectable pancreatic carcinoma. Clin. Cancer. Res. 9, 555-561.
8. van Putten, E.H.P., Kleijn, A., van Beusechem, V.W., Noske, D., Lamers, C.H.J., de Goede, A.L., Idema, S., Hoefnagel, D., Kloezeman, J.J., Fueyo, J. (2022). Convection Enhanced Delivery of the Oncolytic Adenovirus Delta24-RGD in Patients with Recurrent GBM: A Phase I Clinical Trial Including Correlative Studies. Clin. Cancer. Res. 28, 1572-1585.
9. Mantwill, K., Klein, F.G., Wang, D., Hindupur, S.V., Ehrenfeld, M., Holm, P.S., Nawroth, R. (2021). Concepts in Oncolytic Adenovirus Therapy. Int. J. Mol. Sci. 22, 10522.
10. Farrera-Sal, M., Moya-Borrego, L., Bazan-Peregrino, M., Alemany, R. (2021). Evolving Status of Clinical Immunotherapy with Oncolytic Adenovirus. Clin. Cancer. Res. 27, 2979-2988.
11. Burke, S., Shergold, A., Elder, M.J., Whitworth, J., Cheng, X., Jin, H., Wilkinson, R.W., Harper, J., Carroll, D.K. (2020). Oncolytic Newcastle disease virus activation of the innate immune response and priming of antitumor adaptive responses in vitro. Cancer. Immunol. Immunother. 69, 1015-1027.
12. Kakizaki, H., Numasawa, K., Suzuki, K. (1986). Establishment of a new cell line (YTS-1) derived from a human urinary bladder carcinoma and its characteristics. Nihon. Hinyokika. Gakkai. Zasshi. 77, 1790-1795.
13. Todeschini, A.R., Dos Santos, J.N., Handa, K., Hakomori, S.I. (2008). Ganglioside GM2/GM3 complex affixed on silica nanospheres strongly inhibits cell motility through CD82/cMet-mediated pathway. Proc. Natl. Acad. Sci. USA. 105, 1925-1930.
14. Liang, M. (2018). Oncorine, the World First Oncolytic Virus Medicine and its Update in China. Curr. Cancer. Drug. Targets. 18, 171-176.
15. You, R., Xu, Q., Wang, Q., Zhang, Q., Zhou, W., Cao, C., Huang, X., Ji, H., Lv, P., Jiang, H. (2022). Efficacy and safety of camrelizumab plus transarterial chemoembolization in intermediate to advanced hepatocellular carcinoma patients: A prospective, multi-center, real-world study. Front. Oncol. 12, 816198.
16. Stepanenko, A.A., Sosnovtseva, A.O., Valikhov, M.P., Chekhonin, V.P. (2021). A new insight into aggregation of oncolytic adenovirus Ad5-delta-24-RGD during CsCl gradient ultracentrifugation. Sci. Rep. 11, 16088.
17. Liu, M., O'Connor, R.S., Trefely, S., Graham, K., Snyder, N.W., Beatty, G.L. (2019). Metabolic rewiring of macrophages by CpG potentiates clearance of cancer cells and overcomes tumor-expressed CD47-mediated 'don't-eat-me' signal. Nat. Immunol. 20, 265-275.

18. Zirnheld, A.L., Villard, M., Harrison, A.M., Kosiewicz, M.M., Alard, P. (2019). β-Catenin stabilization in NOD dendritic cells increases IL-12 production and subsequent induction of IFN-γ-producing T cells. J. Leukoc. Biol. 106, 1349-1358.
19. Sri-Ngern-Ngam, K., Keawvilai, P., Pisitkun, T., Palaga, T. (2022). Upregulation of programmed cell death 1 by interferon gamma and its biological functions in human monocytes. Biochem. Biophys. Rep. 32, 101369.
20. .Feola, S., Russo, S., Ylösmäki, E., Cerullo, V. (2022). Oncolytic ImmunoViroTherapy: A long history of crosstalk between viruses and immune system for cancer treatment. Pharmacol. Ther. 236, 108103.
21. Annels, N.E., Simpson, G.R., Denyer, M., Arif, M., Coffey, M., Melcher , A., Harrington, K., Vile, R., Pandha, H. (2020). Oncolytic Reovirus-Mediated Recruitment of Early Innate Immune Responses Reverses Immunotherapy Resistance in Prostate Tumors. Mol. Ther. Oncolytics. 20, 434-446.
22. Klawitter, M., El-Ayoubi, A., Buch, J., Rüttinger, J., Ehrenfeld, M., Lichtenegger, E., Krüger, M.A., Mantwill, K., Koll, F.J, Kowarik, M.C., et al. (2022). The Oncolytic Adenovirus XVir-N-31, in Combination with the Blockade of the PD-1/PD-L1 Axis, Conveys Abscopal Effects in a Humanized Glioblastoma Mouse Model. Int. J. Mol. Sci. 23, 9965.
23. Yun, C.O., Hong, J., Yoon, A.R. (2022). Current clinical landscape of oncolytic viruses as novel cancer immunotherapeutic and recent preclinical advancements. Front. Immunol. 13, 953410.
24. Plesca, I., Tunger, A., Müller, L., Wehner, R., Lai, X., Grimm, M.O., Rutella, S., Bachmann, M., Schmitz, M. (2020). Characteristics of Tumor-Infiltrating Lymphocytes Prior to and During Immune Checkpoint Inhibitor Therapy. Front. Immunol. 11, 364.
25. Liu, Z., Ravindranathan, R., Kalinski, P., Guo, Z.S., Bartlett, D.L. (2017). Rational combination of oncolytic vaccinia virus and PD-L1 blockade works synergistically to enhance therapeutic efficacy. Nat. Commun. 8, 14754.
26. Lin, C., Ren, W., Luo, Y., Li, S., Chang, Y., Li, L., Xiong, D., Huang, X., Xu, Z., Yu, Z., et al. (2020). Intratumoral Delivery of a PD-1-Blocking scFv Encoded in Oncolytic HSV-1 Promotes Antitumor Immunity and Synergizes with TIGIT Blockade. Cancer. Immunol. Res. 8, 632-647.
27. Woller, N., Gürlevik, E., Fleischmann-Mundt, B., Schumacher, A., Knocke, S., Kloos, A.M., Saborowski, M., Geffers, R., Manns, M.P., Wirth, T.C., et al. (2015). Viral Infection of Tumors Overcomes Resistance to PD-1-immunotherapy by Broadening Neoantigenome-directed T-cell Responses. Mol. Ther. 23, 1630-1640.
28. Zhang, W., Huang, Q., Xiao, W., Zhao Y., Pi, J., Xu, H., Zhao, H., Xu, J., Evans C.E., Jin, H. (2020). Advances in anti-tumor treatments targeting the CD47/SIRPalpha axis. Front. Immunol. 11, 18.
29. Maute, R., Xu, J., Weissman, IL. (2022). CD47-SIRPα-targeted therapeutics: status and prospects. Immunooncol. Technol. 13, 100070.
30. Zhang, H., Lu, H., Xiang, L., Bullen, J.W., Zhang, C., Samanta, D., Gilkes, D.M., He, J., Semenza, G.L. (2015). Hif-1 Regulates Cd47 Expression in Breast Cancer Cells to Promote Evasion of Phagocytosis and Maintenance of Cancer Stem Cells. Proc. Natl. Acad. Sci. USA. 112, E6215-6223.

31. Advani, R., Flinn, I., Popplewell, L., Forero, A., Bartlett, N.L., Ghosh, N., Kline, J., Roschewski, M., LaCasce, A., Collins, GP., et al. (2018). CD47 Blockade by Hu5F9-G4 and Rituximab in Non-Hodgkin's Lymphoma. N. Engl. J. Med. 379, 1711-1721.
32. Zeidan, A.M., DeAngelo, D.J., Palmer, J., Seet, C.S., Tallman, M.S., Wei, X., Raymon, H., Sriraman, P., Kopytek, S., Bewersdorf, J.P., et al. (2022). Phase 1 study of anti-CD47 monoclonal antibody CC-90002 in patients with relapsed/refractory acute myeloid leukemia and high-risk myelodysplastic syndromes. Ann. Hematol. 101, 557-569.
33. Tseng, D., Volkmer, J.P., Willingham, S.B., Contreras-Trujillo, H., Fathman, J.W., Fernhoff, N.B., Seita, J., Inlay, M.A., Weiskopf, K., Miyanishi, M., et al. (2013). Anti-CD47 antibody-mediated phagocytosis of cancer by macrophages primes an effective antitumor T-cell response. Proc. Natl. Acad. Sci. USA. 110, 11103-11108.
34. Li, W., Wu, F., Zhao, S., Shi, P., Wang, S., Cui, D,. (2022). Correlation between PD-1/PD-L1 expression and polarization in tumor-associated macrophages: A key player in tumor immunotherapy. Cytokine. Growth. Factor. Rev. 67, 49-57.
35. Chen, S.H., Dominik, P.K., Stanfield, J., Ding, S., Yang, W., Kurd, N., Llewellyn, R., Heyen, J., Wang, C., Melton, Z., et al. (2021). Dual checkpoint blockade of CD47 and PD-L1 using an affinity-tuned bispecific antibody maximizes antitumor immunity. J. Immunother. Cancer. 9, e003464.
36. Gauttier, V., Pengam, S., Durand, J., Biteau, K., Mary, C., Morello, A., Néel, M., Porto, G., Teppaz, G., Thepenier, V. (2020). Selective SIRPα blockade reverses tumor T cell exclusion and overcomes cancer immunotherapy resistance. J. Clin. Invest. 130, 6109-6123.
37. Liu, B., Guo, H., Xu, J., Qin, T., Guo, Q., Gu, N., Zhang, D., Qian, W., Dai, J., Hou, S. (2018). Elimination of tumor by CD47/PD-L1 dualtargeting fusion protein that engages innate and adaptive immune responses. MAbs. 10, 315-324.
38. Belcaid, Z., Berrevoets, C., Choi, J., van Beelen, E., Stavrakaki, E., Pierson, T., Kloezeman, J., Routkevitch, D., van der Kaaij, M., van der Ploeg, A., et al. (2020). Low-dose oncolytic adenovirus therapy overcomes tumor-induced immune suppression and sensitizes intracranial gliomas to anti-PD-1 therapy. Neurooncol. Adv. 2, 1-12.

Figures

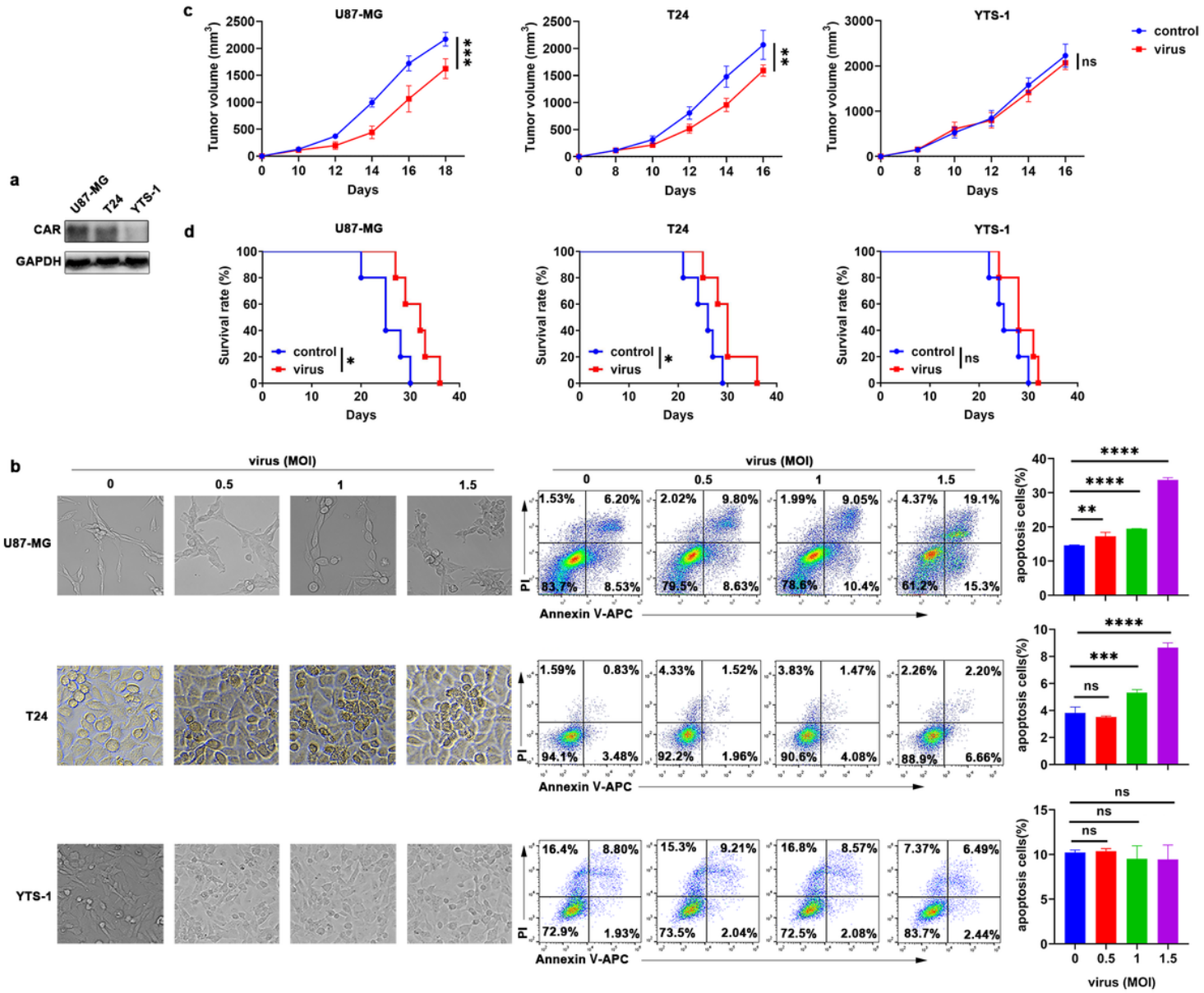

Figure 1

H101 suppress tumor growth by promoting cancer cells apoptosis. a. Western blot of CAR expression in U87-MG, T24 and YTS-1 cells. b. Representative images (left) and annexin V/PI apoptosis detection (right) of U87-MG, T24 and YTS-1 cells stimulated by oncolytic viruses at multiplicity of infection (MOI) of 0.5, 1 or 1.5 for 24 h. c, d. Tumor sizes (c) and mouse survival (d) of tumor-bearing NOD *Prkdc*^{scid} *Il2rg*$^{-/-}$ (NSG) mice inoculated with U87-MG, T24 and YTS-1 cells and received an intratumoral injection of physiological saline solution or H101 (2.5×10^7 pfu per tumor). Representative results from three independent experiments are shown (n = 3 in b; n = 5 in c, d). ns, not significant; *P < 0.05, **P < 0.01, ***P < 0.001, ****P < 0.0001 (unpaired Student's t test: a, b, c; log-rank test: d; mean and s.d.).

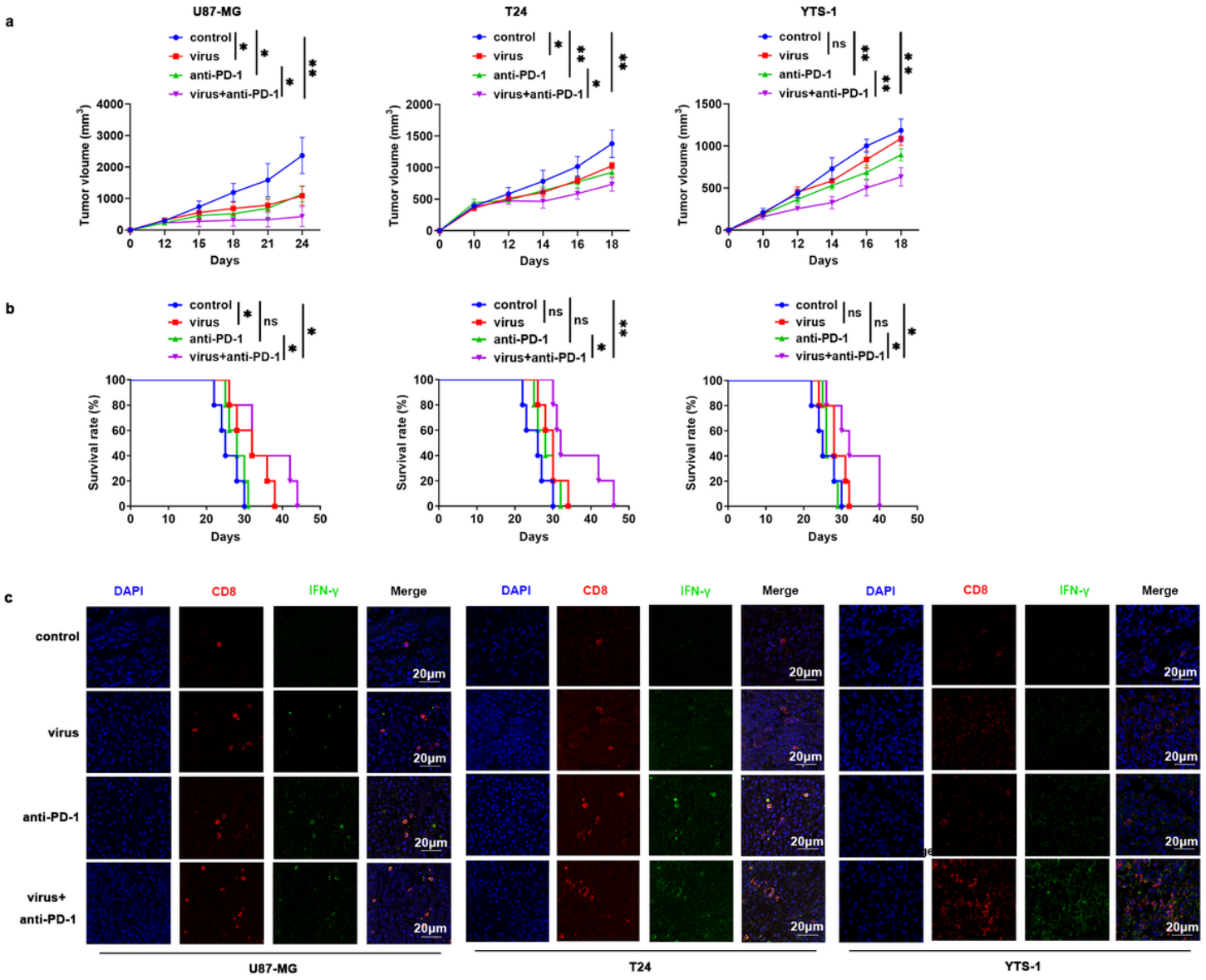

Figure 2

H101 enhance the antitumor effects of anti-PD-1 via increasing IFN-γ. a, b. Tumor sizes (a) and mouse survival (b) of U87-MG, T24 and YTS-1 tumor-bearing NSG mice that received intratumoral transfer of 1×10^6 PBMCs and intratumoral injection of H101 (2.5×10^7 pfu per tumor) every 2 days along with intraperitoneal injection of 50 μg Camrelizumab every 4 days. c, Immunofluorescence analysis of IFN-γ in tumor-infiltrating $CD8^+$ T cells of U87-MG, T24 and YTS-1 tumor-bearing mice that received intratumoral injection of H101 (2.5×10^7 pfu per tumor) every 2 days along with intraperitoneal injection of 50 μg Camrelizumab every 4 days. Representative results from three independent experiments are shown (n = 5 in all statistical groups). ns, not significant; *$P < 0.05$ and **$P < 0.01$ (unpaired Student's *t* test: a; log-rank test: b; mean and s.d.).

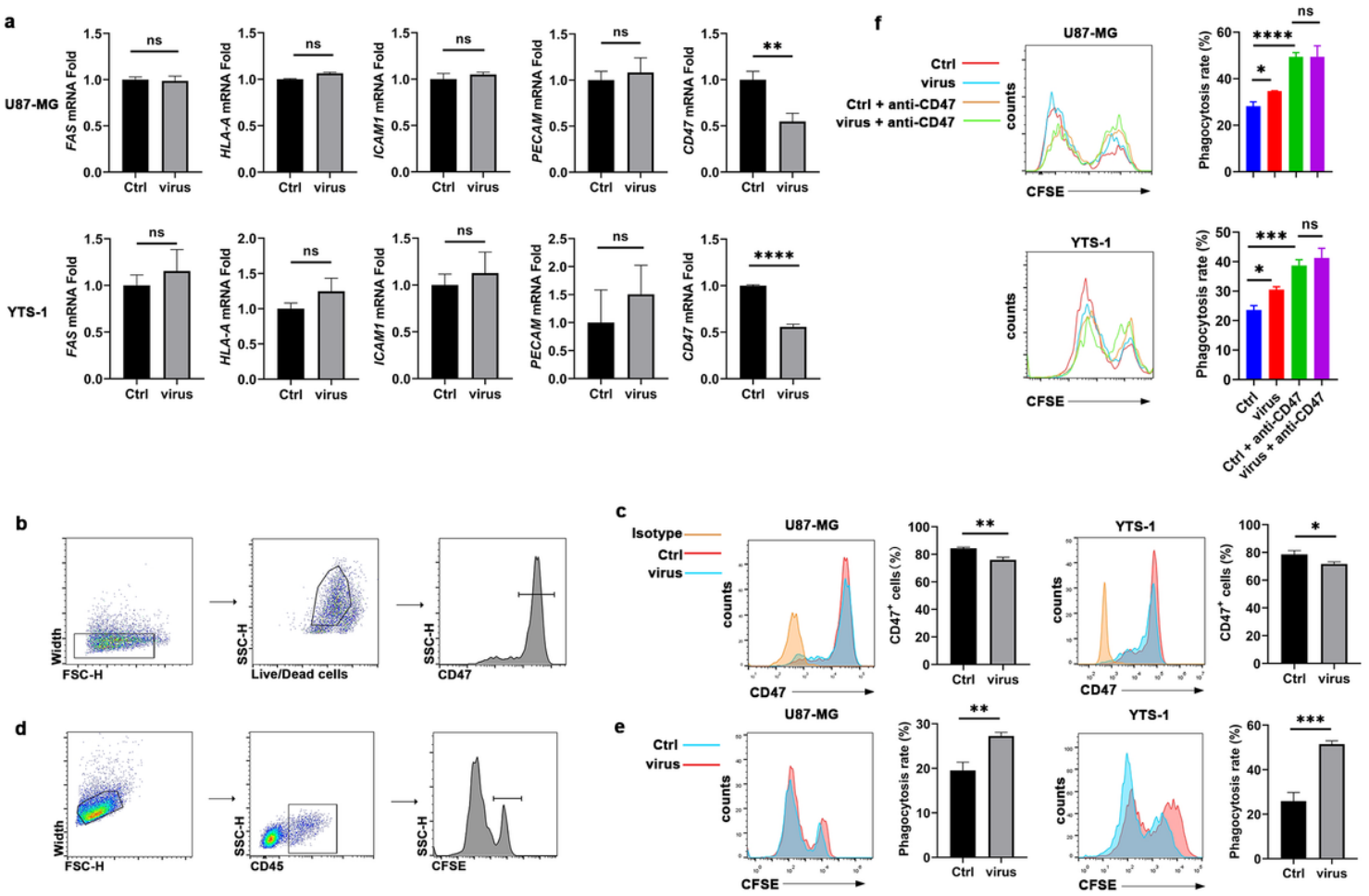

Figure 3

H101 inhibit CD47 expression to induce the macrophage phagocytosis. a. Real-time PCR analysis of FAS, ICAM1, HLA-A, CD47 and PECAM mRNA expression in U87-MG and YTS-1 cells infected by H101 at MOI = 1 for 24 h. b, Gating strategies of Fig. 3c. c, Flow cytometric (FC) analysis of CD47 on U87-MG and YTS-1 cells infected by oncolytic viruses at MOI = 1 for 24 h. d, Gating strategies of Fig. 3e. e. FC analysis of H101-treated (at MOI = 1 for 24 h) U87-MG or YTS-1 cells phagocytosed by induced THP-1 cells cocultured for 8 h. f, FC analysis of phagocytosis of tumor cells treated with oncolytic viruses at MOI = 1 for 24 h cocultured with induced THP-1 cells at the existence of anti-CD47 (10μg/ml).

Representative results from three independent experiments are shown (n = 3 in all statistical groups). ns, not significant; *P< 0.05, **P< 0.01, ***P< 0.001, ****P< 0.0001 (unpaired Student's t test; mean and s.d.).

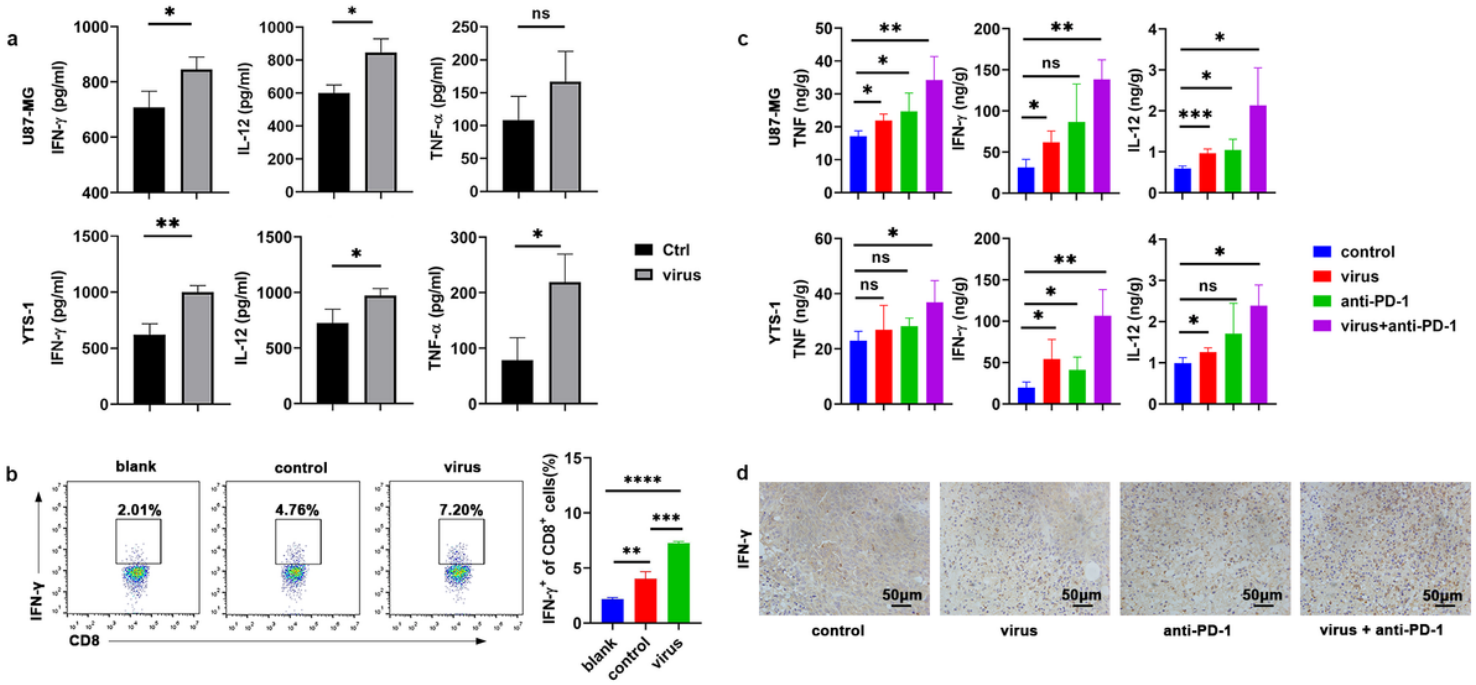

Figure 4

H101-treated tumor cells increased cytokines levels secreted by macrophages to activate T cells. a. Enzyme-linked immunosorbent assay (ELISA) of TNF, IL-12 and IFN-γ secreted by THP-1 cocultured for 24 h with U87-MG or YTS-1 cells treated with H101 at MOI of 1.5 for 24 h. b. FC analysis of the rate of IFN-γ^+ among $CD8^+$ T cells stimulated with supernatants of induced THP-1 cells cocultured with H101-treated (at MOI = 1.5 for 24 h) YTS-1 cells. c. ELISA analysis of TNF-α, IFN-γ and IL-12 levels in tumor tissues of U87-MG and YTS-1 tumor-bearing mice received combination treatment of H101 (2.5×10^7 pfu per tumor) with 50 μg of Camrelizumab. d. Immunohistochemical analysis of IFN-γ in the tumor tissues of YTS-1 tumor-bearing mice received administration of H101 treatment (2.5×10^7 pfu per tumor) along with anti-PD-1 therapy. Representative results from three independent experiments are shown (n = 3 in all statistical groups). ns, not significant; *$P < 0.05$, **$P < 0.01$, ***$P < 0.001$, ****$P < 0.0001$ (unpaired Student's *t* test: a; one-way anova with a turnkey post test: b, c, d; mean and s.d.).

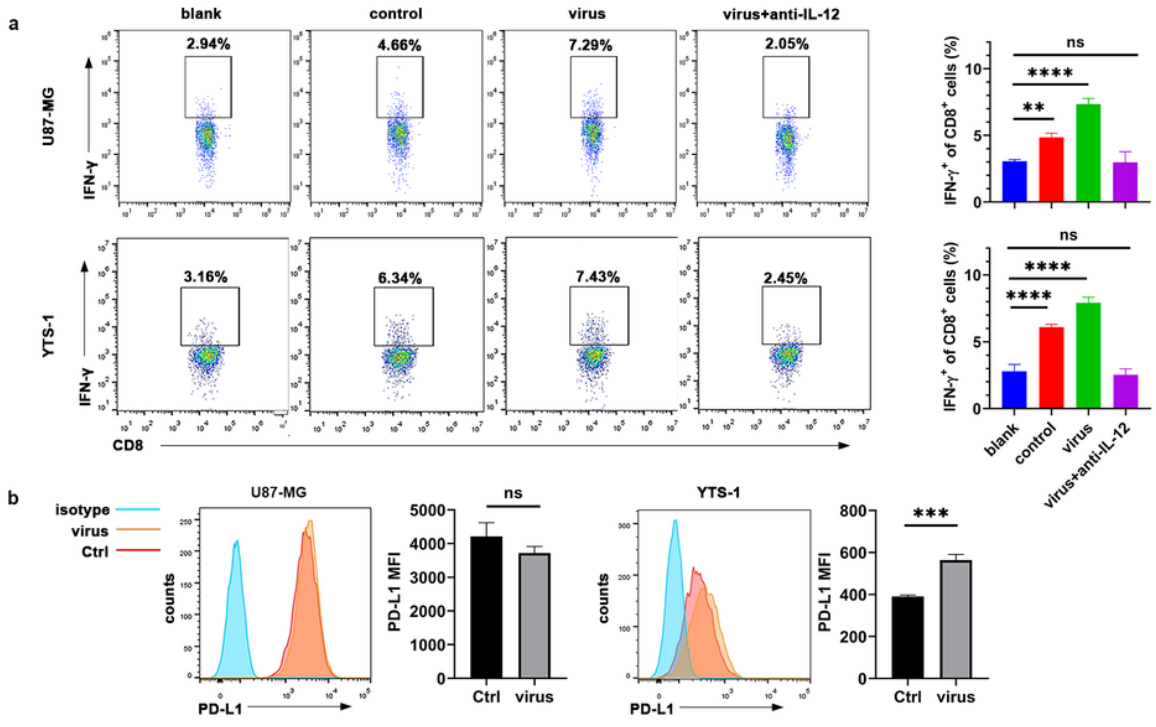

Figure 5

Macrophages promote IFN-γ secretion via IL-12. a. FC analysis of the frequency of $CD8^+IFN\text{-}\gamma^+$ T cells in T cells stimulated by blank T cell medium (blank), supernatants of induced THP-1 (control), supernatants of induced THP-1 phagocytizing oncolytic virus-treated U87-MG or YTS-1 without (virus) or with (virus + anti-IL-12) 10 μg ml^{-1} anti-IL-12 neutralizing antibodies. b. FC analysis of the levels of PD-L1 expressed on U87-MG and YTS-1 cells with H101 treatment at MOI of 1.5 for 24 h. Representative results from three independent experiments are shown (n = 3 in all statistical groups). ns, not significant; $^{**}P < 0.01$ and $^{***}P < 0.001$, $^{****}P < 0.0001$ (one-way anova with a turnkey post test: a; unpaired Student's *t* test: b; mean and s.d.).